JOURNAL OF Applied Polymer SCIENCE

Phase-Dependent Binary Interaction Parameters in Industrial Low-Density Polyethylene Separators

Glória Meyberg Nunes Costa, Yuri Guerrieri, Simão Kislansky, Marcelo Embiruçu
Programa de Engenharia Industrial - Escola Politécnica – Universidade Federal da Bahia, Rua Prof. Aristides Novis, 2, Federação, 40210-630, Salvador, Bahia, Brazil
Correspondence to: M. Embiruçu (E-mail: embirucu@ufba.br)

ABSTRACT: In the production process of low-density polyethylene (LDPE), an important step is the flash separation of monomers and other small molecules from the polymer produced. The process is carried out adiabatically in two stages. To improve the performance of thermodynamic models, it is very important to analyze the use of model binary interaction parameters (BIP) dependent on the phase characteristics for each phase (phase-dependent BIP). In this work the PC-SAFT (perturbed-chain statistical associating fluid theory) equation of state (EOS) is applied to the flash simulation of LDPE industrial separators using eight different resins. The main numerical aspects are examined with emphasis on the optimization strategy for the EOS BIP that explicitly characterizes each phase involved separately. The results demonstrate good predictive behavior. As a result of improved and more consistent modeling, a new strategy for optimized operation can be envisaged for the sequence of separators. © 2013 Wiley Periodicals, Inc. J. Appl. Polym. Sci. 000: 000–000, 2013

KEYWORDS: applications; phase behavior; polyolefins; theory and modeling

Received 3 September 2012; accepted 1 March 2013; Published online
DOI: 10.1002/app.39266

INTRODUCTION

It is a well-known fact that polymerization of ethylene at high pressures takes place at relatively low conversion rates (up to 30%). Therefore, after polymerization and decompression of the reacting mixture, it is necessary to separate the obtained polymer from the unreacted monomer. This is usually carried out in two separating vessels, i.e., high-pressure and low-pressure separators. In order to perform the separation process successfully in the commercial LDPE (low-density polyethylene) unit, the most favorable set-points of pressure and temperature must be chosen and the detailed information on the composition of the phases at equilibrium must be predicted. In a rational design of such pieces of equipment it is necessary to take into account a set of requirements, many of which are often opposite, such as: (a) achieving efficient separation of ethylene from the high molecular weight polymer (b) preventing polymerization of ethylene in the separating vessel, where high temperature and relatively high pressure are maintained (c) avoiding uncontrolled decomposition of ethylene in the separating vessel (d) decreasing the cost of recompression of the ethylene during its recycling as much as possible, which can result in significant energy savings (e) completely avoiding precipitation of low molecular weight polymers in the polymer rich phase as they may impair the quality of the final product and (f) adequate vessel design in order to enable a constant polymer level and intimate contact between the coexisting phases. It is evident that all these requirements cannot be satisfied easily because for those noted in points (a), (b) and (c) low pressure and low temperature are needed, while for others, (d) and (e), an increase in both pressure and temperature are necessary. It is clear from these considerations that the choice of temperature and pressure in the separator is in fact a trade-off of several mutually opposing demands.[1]

With the abundance of thermodynamic models for polymer and polymer solutions, the choice of an appropriate method for a specific application may not be clear. Yet, this choice is crucial for a successful and accurate simulation because it can affect the results considerably. A review of the use of some equations of state (EOS) for LDPE process simulation was presented by Orbey et al.[2] Various equations of state have been proposed and modified to predict polymer-solvent phase behavior. For example, Jog et al.[3] used the SAFT equation of state[4] to describe the phase behavior of the LLDPE + solvent systems investigated by de Loos et al.[5] The Sanchez-Lacombe equation of state[6] was used by Gauter and Heidemann[7] to model the phase behavior of the systems polyethylene + n-hexane and polyethylene + ethylene. A modified Sanchez- Lacombe equation of state[8] was used by Nagy et al.[9] to correlate the phase behavior of the binary

subsystems of ethylene + n-hexane + LLDPE and to predict the phase behavior of the ternary system using parameters obtained from the fit of the binary subsystems. The equation of Sako et al.[10] was used with some success by Tork et al.[11] to calculate the phase equilibrium in binary and ternary systems of polyolefins. Kontogeorgis et al.[12] used the van der Waals EOS to correlate data from vapor-liquid equilibria for polymer solutions. They proposed a method to calculate the equation of state interaction parameter a and the co-volume b for polymers from two volumetric data at low pressure. Orbey and Sandler[13] applied the Peng-Robinson EOS,[14] along with the mixing rules proposed by Wong and Sandler,[15] to correlate vapor-liquid data for some polymer solutions. The SRK EOS, combined with the Flory-Huggins G^E model and the Huron and Vidal[16] mixing rule, was used by Orbey et al.[17] to correlate polymer/solvent vapor-liquid equilibria data. Paricaud et al.[18] correlated the liquid-liquid and vapor-liquid equilibrium of polyethylene-hydrocarbon systems with the SAFT-VR (Statistical Associating Fluid Theory for Potentials of Variable Range) approach and the Flory theory of crystallization. Recently, Costa et al.[19] carried out a detailed evaluation of several activity coefficient models and the activity coefficient from equations of state for the prediction of vapor-liquid and liquid-liquid equilibria for polymer systems both at infinite dilution and finite concentration.

Here the equation of state suggested by Gross and Sadowski[20,21] on the basis of the perturbed-chain statistical associating fluid theory (PC-SAFT) was used to model the polyethylene process separators. The PC-SAFT EOS has been successfully tested on various systems, including nonpolar, polar, and associating substances, as well as polymers and copolymers in a wide range of conditions.[22–26] Some versions of the PC-SAFT model, the original,[20,21] the simplified[27–29] and the group contribution simplified,[29–31] can be applied to polymer systems. The PC-SAFT model has been successfully tested for the modeling of the high and low-pressure separator units in industrial ethylene-polyethylene systems. Buchelli et al.[32] investigated the performance of the PC-SAFT equation of state for modeling the high (HPS) and low-pressure (LPS) separator units downstream from a low-density polyethylene tubular reactor. Plant data were used to validate the equilibrium stage model prediction for the two gas-liquid flash separators, however, the pure component parameters and binary interaction parameters (BIP) of this model were obtained exclusively from experimental data published in the literature. The authors achieved good agreement between the model and LPS plant data, although the predicted solubility for the model was not in agreement with the plant-measured values for the HPS. Modeling and simulation of separation steps in polyethylene plant using the PC-SAFT equation of state was also carried out by Guerrieri.[22] In this work, in addition to the simulation of the LPS process separator with the BIP estimated from industrial experimental data, a simulation of the reactor was also carried out with BIP from literature. Moreover, the performances of SAFT[4] and PC-SAFT[20,21] equations in modeling industrial data were compared. The resulting best model (PC-SAFT) was used later to simulate the behavior of the separator in operational conditions unlike those of typical industrial practice.

Detailed information on the composition of the phases at equilibrium for the wide ranges of temperature and pressure used during the commercial production is scarce for the process engineer. During various upsets in the process, he/she constantly faces problems which cause sudden changes in one or more basic process variables (pressure, temperature and conversion). Although some simulations have been carried out in industrial separators using the PC-SAFT equation of state, there is a need for a new approach to improve the performance of these simulations. Furthermore, as the separators operate in series there is a relationship between the output stream and the feed stream for the following stage of separation. Therefore, if an integrated simulation is devised, and if composition-dependent BIP are used, the BIP have to be different for each phase involved (phase-dependent BIP) in order to assure simulation consistency and also to describe molecular forces that act differently on different phases properly. For example, not only do dielectric constants differ in the liquid and vapour phases, but also the molecular dipole moments. Thus, it is clear that interaction parameters may be expected to differ in the liquid and vapour phases and separate predictions are made for them.[33] The aim of this study is to evaluate industrial simulations taking into account this different approach to BIP as a function of the phase characteristics involved.

PROCESS DESCRIPTION

LDPE is industrially synthesized at relatively high temperatures (180–300)°C and pressures (1000–3000) bar by free-radical bulk polymerization in supercritical ethylene. The high pressure process includes three basic units: (1) a compression unit (2) a reactor, and (3) a separation product system. The polymerization is carried out in a well-stirred single-stage or multistage autoclave or a tubular reactor. In this process, ethylene acts both as a reagent and solvent for the polymer and chain terminator agents (CTA: ethane, propene, and propane) are added in very small quantities with ethylene. Due to the short reactor residence time (30–90 s) the monomer conversion is relatively low, between 10 and 25 wt % in autoclaves and closer 35 wt % in tubular reactors. The reactor effluent stream contains molten polymer, ethylene, and a small amount of unreacted CTA which is depressurized across a pressure reduction valve to allow its subsequent separation. A schematic diagram is shown in Figure 1. The process is carried out adiabatically in two stages. In the first step, the reactor effluent (F2) is depressurized through a pressure reduction valve down to (150–250) bar. This allows the separation of the polymeric product from the unreacted ethylene in the HPS. The overhead monomer rich stream (F4) is cooled and recycled back to the reactor, whereas the bottom polymer rich stream (F3) undergoes a second separation step at a near atmospheric pressure in the LPS. The overhead stream of LPS (F6) is recycled back to the reactor, while the residual ethylene and comonomers dissolved in the molten polymer (F5) may be stripped under vacuum conditions in a devolatilizing extruder. One of the most important issues in the design of these flash separators is the prediction of the amount of monomer left in the final product. The presence of monomer in the

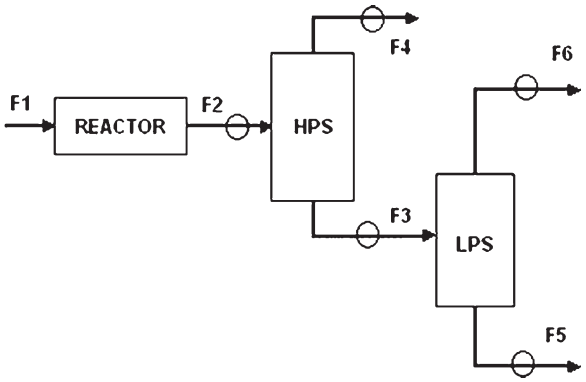

Figure 1. Simplified flowsheet of a LDPE plant.

polymer is undesirable for several reasons and should be minimized.

PC-SAFT EQUATION OF STATE

The PC-SAFT EOS is based on a perturbation theory where the hard-chain reference term represents the repulsive forces and the perturbation terms reflect the various attractive interactions, as described in detail elsewhere.[20,21] For associating fluids, this EOS is conveniently written in terms of the reduced residual Helmholtz free energy as follows:

$$\frac{A^{res}}{N\cdot k\cdot T}=\frac{A^{hc}}{N\cdot k\cdot T}+\frac{A^{disp}}{N\cdot k\cdot T}+\frac{A^{assoc}}{N\cdot k\cdot T} \quad (1)$$

where A is the Helmholtz free energy per number of molecules, N is the total number of molecules, k is the Boltzmann constant, superscripts *res*, *hc*, *disp*, and *assoc* identify the residual, the hard-chain, the dispersive attraction and the associative attraction contributions, respectively. All the required expressions for these terms in eq. (1), as well as the pure-component parameters for many substances, can be found in the literature.[20,21] When PC-SAFT is used for mixtures, the conventional Berthelot-Lorenz combining rules used to calculate the mixture properties in the hard-chain and the dispersion terms are applied, introducing only one adjustable BIP to account for the dispersive interactions, as follows:

$$\sigma_{ij}=\frac{1}{2}\cdot\left(\sigma_i+\sigma_j\right) \quad (2)$$

$$\varepsilon_{ij}=\sqrt{\varepsilon_i\cdot\varepsilon_j}\cdot\left(1-k_{ij}\right) \quad (3)$$

where σ is the segment diameter and ε is the dispersion energy parameter.

RESULTS AND DISCUSSION

Pure Component Parameters and BIP Fitting Criteria

The pure component parameters and segment parameters of the polymer for the PC-SAFT EOS are taken from literature[20,21] and are shown in Table I, where m is the segment number, σ is the segment diameter, and ε/K is the association energy.

Generally, data from literature are used to estimate BIP. However, at high pressure, experimental data from literature are scarce and simulation results using only these data are less accurate. Thus industrial operational plant data were used here to estimate BIP and the Nelder-Mead simplex method[34] is applied to minimize the following objective function:

$$OF=\sum_{i=1}^{nc}\left(\frac{w'^{calc}_i-w'^{exp}_i}{w'^{exp}_i}\right)^2+\sum_{i=1}^{nc}\left(\frac{w''^{calc}_i-w''^{exp}_i}{w''^{exp}_i}\right)^2 \quad (4)$$

where the superscripts calc and exp are related to the calculated and experimental values, respectively, w'_i is the mass composition of component i in the heavy phase, w''_i is the mass composition of component i in the light phase and nc is the number of components.

Regarding polymer phase equilibrium calculations, the component composition is usually presented as a mass fraction because the polymer has a much higher molecular weight than the solvent. The equation of state is defined in terms of molar fractions, which can lead to numerical problems for computing the polymer molar fraction as it becomes very small. A similar problem may occur when modeling polymer vapor-liquid equilibrium: in the gas phase, there is almost no polymer, but thermodynamically this value cannot be zero, even though it may be extremely low. Some difficulties for calculating phase equilibrium in flash separators arise from these features, such as the influence of mass and mole composition on the phase equilibrium, the general optimization strategy for the estimation of the EOS interaction parameters, the algorithms of flash calculation, the influence of low and high polymer concentration, and the convergence criteria at each step of the calculation. The reader is encouraged to refer to Costa et al.[35] in order to see some numerical approaches to overcome these difficulties.

Experimental Data Conditions

Circles in Figure 1 identify streams used in this study. Stream F1 contains ethylene and small amounts of propene and propane and feeds the reactor. The discharge stream (F2) containing ethylene, polymer, a small amount of ethane (formed in the reaction), propene, and propane, is sent to the HPS. The HPS bottom stream (F3) is sent to the LPS. The LPS top stream (F6) returns to the process and its bottom stream (F5), containing essentially pure polymer, is sent to the extruder. The following experimental data are necessary to validate the HPS model: F2, T_{HPS}, P_{HPS} and z_{HPS} (input data); F3, x_{HPS}, F4 and y_{HPS} (output

Table I. Pure Component Parameters for PC-SAFT Equation of State

	M	σ	ε/k
Component	(-)	(Å)	(K)
Ethylene	1.5930	3.4450	176.47
Ethane	1.6069	3.5206	191.42
Propene	1.9597	3.5356	207.19
Propane	2.0020	3.6184	208.11
LDPE	$0.0263\cdot Mw$	4.0217	249.50

Table II. LDPE Density and Molecular Weight and Separators Operational Conditions

Resin	ρ (g/cm^3)	M_w (kg/mol)	M_n (kg/mol)	PDI	T_{HPS} (°C)	P_{HPS} (bar)	T_{LPS} (°C)	P_{LPS} (bar)
LDPE-1	0.921	335	23.1	14.50	280.29	250.06	241.04	0.35
LDPE-2	0.921	295	25.9	11.40	278.80	251.90	239.49	0.42
LDPE-3	0.922	181	23.1	7.84	230.29	249.88	212.17	0.37
LDPE-4	0.923	166	21.8	7.61	253.03	250.55	226.73	0.46
LDPE-5	0.918	340	20.0	17.00	237.68	249.87	217.91	0.42
LDPE-6	0.921	322	28.2	11.42	277.17	249.54	242.73	0.41
LDPE-7	0.918	237	11.9	19.88	247.92	254.00	224.93	0.40
LDPE-8	0.921	426	16.5	25.84	265.33	253.28	235.69	0.42

data), where z_{HPS}, x_{HPS} and y_{HPS} are the mass composition of the feed, bottom and top streams, respectively, F2, F3 and F4 are the total mass flow at the feed, bottom and top streams, respectively, and T_{HPS} and P_{HPS} are the HPS operational temperature and pressure, respectively. Similarly, the following experimental data are needed to validate the LPS model: F3, T_{LPS}, P_{LPS} and z_{LPS} (equal to x_{HPS}) (input data); F5, x_{LPS}, F6 and y_{LPS} (output data), where z_{LPS}, x_{LPS} and y_{LPS} are the mass composition of the feed, bottom and top streams, respectively, F3, F5 and F6 are the total mass flow at the feed, bottom and top streams, respectively, and T_{LPS} and P_{LPS} are the LPS operational temperature and pressure, respectively. Experimental data of flow, temperature and pressure were obtained from plant measurements. Some compositions were measured by on-line gas chromatograph and others were obtained through data reconciliation, although it was still necessary to assume some hypotheses, such as the absence of polymer in stream F6 and the consideration that stream F5 is composed of pure polymer. Data were collected at steady state, but there are some fluctuations which can never be completely avoided when dealing with industrial plant data. To cope with these, the data were collected in triplicate and an appropriate average was extracted from this data set. Further details involved in collecting and treating the industrial data are described elsewhere.[22,36]

We selected eight resins to study the several aspects of LDPE flash separation. Table II shows the HPS and LPS operational conditions and the characteristics of the resins, including solid polymer density (ρ, an inverse and indirect measurement of the degree of branching), polydispersity index (PDI) and weight (M_w), and number (M_n) average molecular weights. In order to present sufficient information to follow the simulation problem Table III shows the feed range composition of the HPS and LPS separators and Tables IV and V show the compositions of all the streams for each resin.

Simulation Results

The polymer is assumed to be monodisperse for all systems because the molar masses are high and because molecular weight distribution (MWD) data are available only for resins LDPE-1 and LDPE-6. This assumption is also due to the negligible effect of polydispersity on the overall model performance, previously investigated and shown in Costa et al.[36] where the polymer was discretized into 5 pseudo-components. They concluded that there is no significant difference between model predictions and plant data for both monodisperse and polydisperse polymers. The only advantage noted in considering a polymer polydisperse instead of monodisperse is an evaluation of the wax composition obtained in the top separator. In addition, the density data presented in Table II show that the effect of the degree of branching is probably small in the systems analyzed here. As shown in Equation (5), weight-average molar masses were used in the calculations and, as stated earlier, the pure component parameters and segment parameters of the polymer for the PC-SAFT EOS are taken from literature.[20,21]

Overall BIP Estimated for the LPS and HPS Simulations. Using the above-mentioned calculation method the BIP (LDPE-solvents) required to fit the industrial data for each LDPE resin was obtained. The calculated values are shown in Table VI for the low and high pressure separators for each LDPE resin. These BIP are the same for LDPE + (solvent: monomers and all small molecules), and all the other BIP were set to zero.

There are two physical reasoning we can use to explain the different values obtained for the BIP at high and low pressures: (i) one way is to analyze the BIP considering their effect on interaction energy, through their relative values (ii) and the other is to analyze these results as a consequence of "ideal mixing" deviations, represented by BIP absolute values. The analysis of these two rationales is controversial and sometimes even conflicting due to complex interactions arising from the different chemical nature (though this difference is not observed in the systems analyzed here) of the components, in addition to differences in size and shape, and also from the different pressure and

Table III. LPDE Feed Range Composition in the HPS and LPS Separators

	HPS		LPS	
	Min	Max	Min	Max
Ethylene	73.4	77.0	20.7	25.9
Ethane	0.3	2.6	0.1	0.8
Propene	0.0	0.2	0.0	0.1
Propane	0.0	1.6	0.0	0.5
LDPE	19.5	25.5	72.9	79.2

Table IV. Mass Fractions of Ethylene, Ethane, Propene, Propane, and LDPE of all the Streams: LDPE Resins 1 to 4

Stream	Ethylene	Ethane	Propene	Propane	LDPE
LDPE-1					
F2	74.30	0.26	0.01	0.04	25.39
F3	20.83	0.07	0.00[a]	0.01	79.08
F4	99.59	0.35	0.01	0.05	0.00
F5	0.00	0.00	0.00	0.00	100.00
F6	99.59	0.35	0.01	0.05	0.00
LDPE-2					
F2	74.07	0.37	0.02	0.04	25.50
F3	20.70	0.10	0.01	0.01	79.18
F4	99.42	0.49	0.03	0.05	0.00
F5	0.00	0.00	0.00	0.00	100.00
F6	99.42	0.49	0.03	0.05	0.00
LDPE-3					
F2	73.82	0.95	0.01	0.01	25.21
F3	20.80	0.27	0.00[b]	0.00[c]	78.92
F4	98.70	1.27	0.01	0.02	0.00
F5	0.00	0.00	0.00	0.00	100.00
F6	98.70	1.27	0.01	0.02	0.00
LDPE-4					
F2	74.26	0.59	0.01	0.01	25.14
F3	20.96	0.17	0.00[d]	0.00[e]	78.87
F4	99.20	0.78	0.01	0.01	0.00
F5	0.00	0.00	0.00	0.00	100.00
F6	99.20	0.78	0.01	0.01	0.00

[a] 2.31×10^{-3}.
[b] 2.64×10^{-3}.
[c] 3.62×10^{-3}.
[d] 1.89×10^{-3}.
[e] 2.98×10^{-3}.

temperature levels (although this variable does not present levels appreciably different here).

Considering the effect on interaction energy, from the mixing rule [eq. (3)], a negative k_{ij} results in a higher interaction energy, i.e., interactions are greater at higher pressures. The positive sign gives out a lower interaction energy at lower pressures, which is consistent with the fact that stronger polymer-solvent interactions are more common at high pressures than at atmospheric pressure (as in LPS).

From another point of view, the absolute value of k_{ij} represents the deviations from "ideal mixing," which depends on differences in molecular size and intermolecular forces. For the systems analyzed the intermolecular forces may be considered to be similar regarding the chemical nature of their components. Thus, "ideal mixing" deviations are related mainly to molecular size differences through the different molecular weights of the polymer and the resulting molecular rearrangements. Therefore, the molecular weight is the variable that most influences the BIP of the systems analyzed. In this case, in the comparison between LPS and HPS, BIP shows smaller absolute values for HPS. This result is an indication that there is a greater "ideal mixing" deviation in LPS than in HPS. This may be because the pressure is substantially lower in LPS, and when the pressure is low there is a substantial mobility of the molecules in the liquid phase, allowing a large number of polymer arrangements and consequently a greater "ideal mixing" deviation. As will be shown later, the overall BPI is greatly influenced by the liquid phase interactions because, given the increased non ideality of this phase compared to the vapor phase, not considering liquid phase binary interactions produces more errors in eq. (4) than disregarding binary interactions in the vapor phase does.

Phase-Dependent BIP Estimated for the LPS and HPS Simulations. The BIP (LDPE-solvents) for each phase (kl_{ij} for liquid phase and kv_{ij} for vapor phase) required to fit the experimental data for each LDPE resin are shown in Table VII for LPS. As explained earlier, when comparing the BIP values exhibited in Table VI with the kl_{ij} values in Table VII, no significant difference is observed. The same comparisons with the kv_{ij} values demonstrate that there is no similarity between these values and the overall BIP values.

Table V. Mass Fractions of Ethylene, Ethane, Propene, Propane, and LDPE of all the Streams: LDPE Resins 5 to 8

Stream	Ethylene	Ethane	Propene	Propane	LDPE
LDPE-5					
F2	77.03	1.86	0.01	1.58	19.52
F3	25.90	0.63	0.00	0.53	72.94
F4	95.71	2.31	0.01	1.97	0.00
F5	0.00	0.00	0.00	0.00	100.00
F6	95.71	2.31	0.01	1.97	0.00
LDPE-6					
F1	98.79	1.17	0.03	0.02	0.00
F2	74.26	1.36	0.02	0.02	24.33
F3	21.46	0.39	0.01	0.00[a]	78.13
F4	98.15	1.80	0.03	0.02	0.00
F5	0.00	0.00	0.00	0.00	100.00
F6	98.15	1.80	0.03	0.02	0.00
LDPE-7					
F2	73.45	2.55	0.19	0.58	23.23
F3	21.94	0.76	0.06	0.17	77.07
F4	95.67	3.33	0.25	0.76	0.00
F5	0.00	0.00	0.00	0.00	100.00
F6	95.67	3.33	0.25	0.76	0.00
LDPE-8					
F2	75.17	1.73	0.03	0.59	22.48
F3	22.97	0.53	0.01	0.18	76.32
F4	96.97	2.23	0.03	0.76	0.00
F5	0.00	0.00	0.00	0.00	100.00
F6	96.97	2.23	0.03	0.76	0.00

[a] 4.80×10^{-3}.

Table VI. Overall BIP Used for LPS and HPS Simulations (LDPE Resins with Any Solvent)

Resin	LPS k_{ij}	HPS k_{ij}
LDPE-1	0.1323	−0.0643
LDPE-2	0.1393	−0.0611
LDPE-3	0.1764	−0.0448
LDPE-4	0.1037	−0.0545
LDPE-5	0.1594	−0.1068
LDPE-6	0.1159	−0.0772
LDPE-7	0.1713	−0.0720
LDPE-8	0.1361	−0.0870

Table VII also displays the values of the estimated BIP for the liquid (kl_{ij}) and vapor (kv_{ij}) phases for the HPS. The same behavior observed in LPS is detected in HPS, i.e., there is a great resemblance between the overall (k_{ij}) and liquid phase (kl_{ij}) BIP values. As can be seen in Table VII there is a marked difference between the values of the interaction parameters when considering the liquid (kl_{ij}) and vapor phases (kv_{ij}) separately. This difference corroborates the importance of considering different BIP for the two phases in equilibrium.

There are two possible conceptual assessments of the behavior expressed by the BIP values in Table VII. Regarding the effect on interaction energy (evaluated by BIP relative values), the same considerations concerning overall BIP apply to phase-dependent BIP. In both LPS and HPS, $kv_{ij} < kl_{ij}$, i.e., interactions are stronger in the vapor phase. Moreover, as kv_{ij} (HPS) $< kv_{ij}$ (LPS), the vapor phase interactions are higher in HPS (in agreement with common knowledge). Likewise, kl_{ij} (HPS) $< kl_{ij}$ (LPS) implies that interactions are greater at higher pressures, which is also a reasonable interpretation.

On the other hand, an "ideal mixing" deviation analysis (evaluated by BIP absolute values) can also be performed. Concerning the similarity of the overall BIP values (k_{ij}) and the liquid phase BIP values (kl_{ij}) for the two separators, this behavior can be credited to the fact that most of the composition of the liquid phase consists of polymer. This apparently seems to be an important factor when considering the ideality deviation as arising from several possible molecular arrangements. Therefore, as stated earlier, the nonideality of the liquid phase is greater than the nonideality of the vapor phase and thus the mass composition errors of the former are greater and exert more influence over the objective function (OF) expressed by eq. (4). As the same OF is used either to obtain the overall BIP or the phase-dependent BIP, the overall BIP values (k_{ij}) tend to be naturally close to the liquid phase BIP values (kl_{ij}).

Now we analyze the difference between the liquid (kl_{ij}) and vapor (kv_{ij}) phases BIP values for LPS displayed in Table VII. As stated earlier, in low pressure conditions the molecules mobility in the liquid phase is significant, resulting in a greater number of polymer arrangements. In the vapor phase the molecules have higher mobility. However, due to the fact that the components have similar molecular structures (polymer content is negligible) and they are more distant from each other than the molecules of the liquid phase, their interactions are weaker, and consequently $|kl_{ij}| > |kv_{ij}|$. On the other hand, an opposite effect is observed in HPS as shown in Table VII. Here even though the polymer is presented in larger quantities in the liquid phase, the probability of different molecular arrangements is much lower because the pressure is too high. The term "packaging" can be used to express this behavior and consequently these compact molecular arrangements. Moreover, the high pressure in HPS induces an increase in the number of interactions between the molecules in vapor phase which causes a pronounced effect on kv_{ij}. As a result, $|kl_{ij}| < |kv_{ij}|$ in HPS.

Correlations for Overall and Phase-Dependent BIP in the LPS and HPS Simulations. BIP of EOS are usually estimated considering only temperature dependence, but for polymer it is possible to develop BIP correlations with temperature, composition and molecular weight as independent variables. For polymer systems, parameters dependence on mixture composition cannot be neglected[37–39] and should take into account the segment interactions and their molecular displacements. Wohlfarth and Rätzsch[40] present a detailed discussion of the dependence of interaction parameters on temperature, composition and molecular weight distribution. However, a typical problem that appears is the choice of the reference composition (feed, top or bottom). As the separator feed composition changes less than that of the top and bottom streams, it is more consistent to assume that the parameters depend on feed composition.[37–41] This approach works well if the two separators are being considered independently, but inconsistencies in stability tests and

Table VII. Phase-Dependent BIP Used for LPS Simulation (LDPE Resins with Any Solvent)

Resin	LPS k_{ij} (Table VI)	LPS kl_{ij}	LPS kv_{ij}	HPS k_{ij} (Table VI)	HPS kl_{ij}	HPS kv_{ij}
LDPE-1	0.1323	0.1322	−0.0120	−0.0643	−0.0630	−0.1526
LDPE-2	0.1393	0.1393	−0.0128	−0.0611	−0.0589	−0.1380
LDPE-3	0.1764	0.1837	−0.0137	−0.0448	−0.0405	−0.0938
LDPE-4	0.1037	0.1025	−0.0142	−0.0545	−0.0518	−0.1108
LDPE-5	0.1594	0.1589	−0.0150	−0.1068	−0.0935	−0.1989
LDPE-6	0.1159	0.1127	−0.0152	−0.0772	−0.0718	−0.1337
LDPE-7	0.1713	0.1714	−0.0163	−0.0720	−0.0589	−0.1456
LDPE-8	0.1361	0.1361	−0.0125	−0.0870	−0.0774	−0.1784

Table VIII. Constants for Overall and Phase-Dependent BIP Used with LPS and HPS Simulations (LDPE Resins with any Solvent)

Constant	k_{ij}	kl_{ij}	kv_{ij}
α [atm]	$-1.80\ 10^{2}$	$-1.89\ 10^{2}$	–
β [atm · mol^2 · kg^{-2}]	–	$1.33\ 10^{3}$	–
δ [atm · mol^2 · kg^{-2}]	–	$6.88\ 10^{1}$	$1.44\ 10^{3}$
η [atm · mol^3 · kg^{-3}]	–	$-1.13\ 10^{1}$	–
γ [atm]	$-1.44\ 10^{3}$	$-1.58\ 10^{3}$	$4.88\ 10^{3}$
λ [mol · kg^{-1}]	$3.26\ 10^{0}$	–	–
Θ [–]	–	–	$-9.64\ 10^{4}$
ω [–]	–	–	$9.57\ 10^{2}$

energy balances arise in simulation of integrated piece of equipment because the HPS liquid withdrawn is the feed to the LPS and the BIP associated with this liquid stream changes and so too the thermodynamic properties. In such situations we can consider a different BIP for each phase, which would overcome these problems (this approach would be also in agreement with G^E-based mixing rules, which are thermodynamically consistent models and where the BIP are indirectly related to the composition of each phase). Although this procedure is more involved numerically, it brings a more consistent theoretical framework. Therefore, BIP values were correlated as a function of polymer molecular weight, outlet composition, and pressure (since temperature variations are not sufficiently informative).

In order to show the predictive ability of PC-SAFT with these correlations, 5 resins (1, 2, 4, 7, and 8) among the 8 investigated resins were randomly chosen to estimate a correlation for the BIP and the other 3 resins (3, 5, and 6) were used to evaluate the prediction capability of this correlation. The target is to determine a unique correlation for the liquid phase parameter appropriate for the two separators simultaneously as well as a single one for the vapor phase. Therefore, with the five resins mentioned above, the parameters for the vapor phase of the two separators were simultaneously merged, based on running a Nelder-Mead optimization simultaneously on all 10 systems to adjust the parameters. A similar approach was used for the liquid phase with the same selected systems. Several attempts have been made to establish a connection between BIP and the molecular weight of the resin, pressure and outlet composition in LPS and HPS. The following equation was found to be suitable for the liquid phase:

$$kl_{ij}=\frac{\alpha+X1+\beta\cdot X2^2}{\gamma+\delta\cdot X2^2+\eta\cdot X2^3} \tag{5}$$

where $X1=P$, $X2=Mw\cdot 10^{-3}/\%Pol$, P is the pressure (atm), Mw is the weight average molecular weight, $\%Pol$ is the polymer percentile weight in liquid phase, whereas the following one for vapor phase:

$$kv_{ij}=\frac{\omega+X3}{\theta+\delta\cdot X1^2+\frac{\gamma}{X1}} \tag{6}$$

where $X1=P$, $X3=\%Ethyl/\%Etha$, $\%Ethyl$ and $\%Etha$ are the ethylene and ethane percentile weight in the vapor phase composition respectively. The values of the constants of eqs. (5) and (6) are shown in Table VIII. It is important to highlight the need to use the composition of the most concentrated component as an independent variable because these correlations are extremely sensitive to variations around low composition variables due to convergence problems, and also to highlight the thermodynamic consistency of using pressure-dependent BIP, as shown in Appendix A.

In order to make a fair comparison between the overall and phase-dependent approaches, a correlation was also developed for the estimated overall BIP:

$$k_{ij}=\frac{\alpha+X1}{\gamma+\lambda\cdot X2} \tag{7}$$

where $X1=P$, $X2=Mw\cdot 10^{-3}/\%Pol$, P is the pressure (atm), Mw is the weight average molecular weight, $\%Pol$ is the polymer percentile weight in the liquid phase. The values of the constants of eq. (7) are also shown in Table VIII. It must also be emphasized that all the correlations do reduce to an ideal mixing state at limit conditions (i.e., k_{ij} tends to zero at very low pressure and polymer concentration, which also means low molecular weight), as shown by eq. (8).

$$\begin{aligned}&\lim_{\substack{P\to 0\\(X1\to 0)\\\%Pol\to 0\\(X2\to\infty)}}\left(\frac{\alpha+X1+\beta\cdot X2^2}{\gamma+\delta\cdot X2^2+\eta\cdot X2^3}\right)\\&=\lim_{\substack{P\to 0\\(X1\to 0)}}\left(\frac{\omega+X3}{\theta+\delta\cdot X1^2+\frac{\gamma}{X1}}\right)\\&=\lim_{\substack{P\to 0\\(X1\to 0)\\\%Pol\to 0\\(X2\to\infty)}}\left(\frac{\alpha+X1}{\gamma+\lambda\cdot X2}\right)=0\end{aligned} \tag{8}$$

At this stage we can compare the simulations from the thermodynamic framework described above with the overall BIP approach and the plant measurements for the LPS. Figure 2 shows the comparison of the model predictions and the plant measurements of the overhead ethylene composition. This assessment involves the use of four different approaches: overall (Table VI) and phase-dependent (Table VII) estimated BIP for each resin, and the developed correlations, expressed by eqs. (5), (6), and (7), where only five resins were used for the adjustment.

From Figure 2 and Table IX we can conclude that the phase-dependent BIP correlations expressed by eqs. (5) and (6) and the overall correlation expressed by eq. (7) are quite adequate, although the difference between using phase-dependent BIP versus overall BIP is not clearly noticeable when expressed in terms of phase composition (liquid compositions are not shown since the liquid phase is almost pure polymer). Another point to be highlighted is the quality of the vapor phase correlation

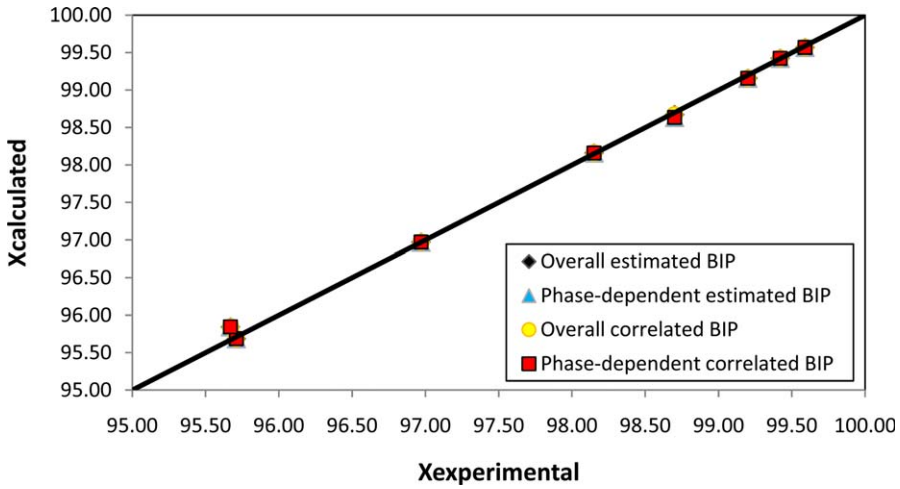

Figure 2. LPS overhead ethylene composition. Experimental and predicted data using overall and phase-dependent estimated and correlated BIP. [Color figure can be viewed in the online issue, which is available at wileyonlinelibrary.com.]

expressed by eq. (6) despite the fact that it encompasses binary interactions at low and high pressure levels.

Table IX shows that for LPS there is no correlation between the magnitude of the errors and the fact that the system has been used or not in developing the correlation. That is, the modeling error for the top compositions of ethane and ethylene are independent of the estimation procedure as well as the fact that the resins have been selected to fit or not (the case of resins 3, 5, 6).

Figures 3–5 and Tables X and XI show the comparison of the model predictions and the plant measurements of the overhead and bottom polymer and ethylene compositions in the HPS, again with the four different approaches: overall (Table VI) and phase-dependent (Table VII) estimated BIP, and the developed correlations, eqs. (5), (6), and (7). There is one important difference between this evaluation and the preceding one (LPS). The results show that when the simulation is performed using an overall BIP there is a systematic underestimation regarding the experimental value for ethylene and polyethylene in the bottom stream. With regard to ethylene in the overhead there is an overestimated composition when compared with the experimental value. Since the polymer is the most important component in the process, an underestimation of this composition leads to a performance calculation yield lower than the real operation one. Furthermore, ethylene, which is also underestimated by the model, when in excess hampers the transport of polymer to the extruder and creates an explosive environment in the storage silos.

Another important problem that can be observed when using overall BIP is related to ethylene behavior in HPS overhead. As the calculated amount is higher than the experimental value, the amount of fresh ethylene to be added to the reactor would

Table IX. LPS Overhead Ethane and Ethylene Model C**omposition** Errors[a]

	Overall estimated BIP (Table VI)		Phase-dependent estimated BIP (Table VII)		Overall correlated BIP [eq. (7)]		Phase-dependent correlated BIP [eqs. (5) and (6)]	
Resin	Etha[b]	Ethyl[c]	Etha[b]	Ethyl[c]	Etha[b]	Ethyl[c]	Etha[b]	Ethyl[c]
LDPE-1	4.40	0.02	4.40	0.02	4.40	0.02	4.40	0.02
LDPE-2	1.98	0.00	1.98	0.00	1.98	0.00	1.98	0.00
LDPE-3	−0.85	0.03	−0.80	0.07	−0.82	0.07	−0.82	0.07
LDPE-4	−3.11	0.04	−3.09	0.04	−3.11	0.04	−3.11	0.04
LDPE-5	−0.76	0.02	−0.76	0.02	−0.76	0.02	−0.76	0.02
LDPE-6	0.90	−0.01	0.91	−0.01	0.90	−0.01	0.90	−0.01
LDPE-7	0.30	−0.18	0.30	−0.18	0.30	−0.18	0.30	−0.18
LDPE-8	−0.33	0.00	−0.33	0.00	−0.34	0.00	−0.33	0.00

[a] *error*[%] = 100 (*exp* − calc)/exp.

[b] Ethane.

[c] Ethylene.

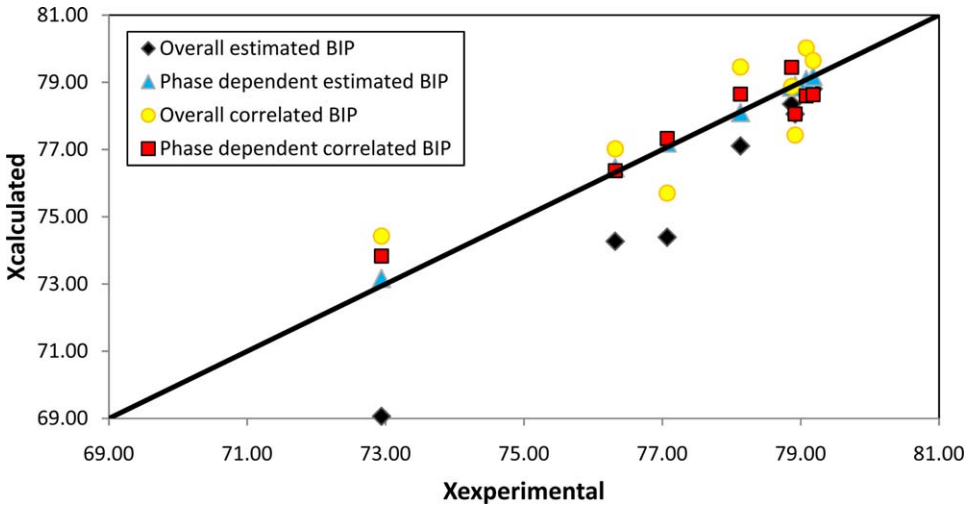

Figure 3. HPS bottom polymer composition. Experimental and predicted data using overall and phase-dependent estimated and correlated BIP. [Color figure can be viewed in the online issue, which is available at wileyonlinelibrary.com.]

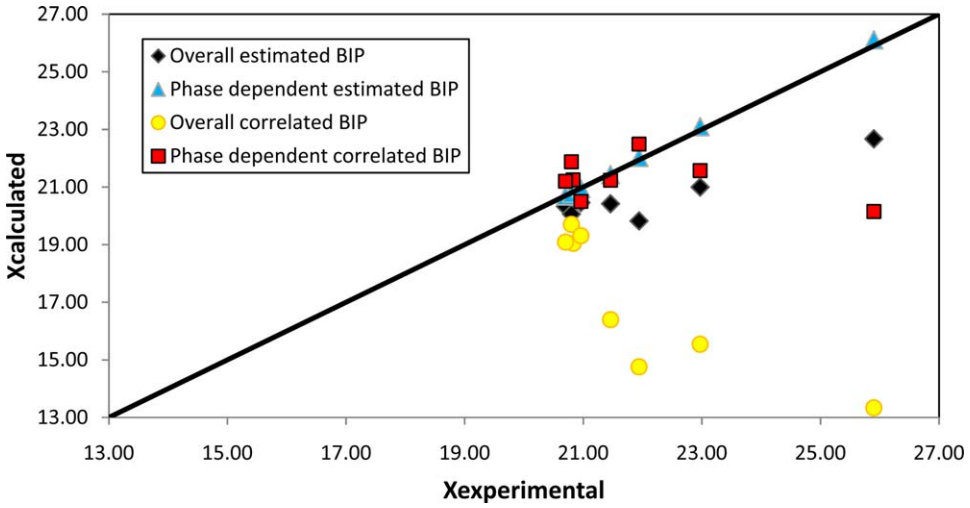

Figure 4. HPS bottom ethylene composition. Experimental and predicted data using overall and phase-dependent estimated and correlated BIP. [Color figure can be viewed in the online issue, which is available at wileyonlinelibrary.com.]

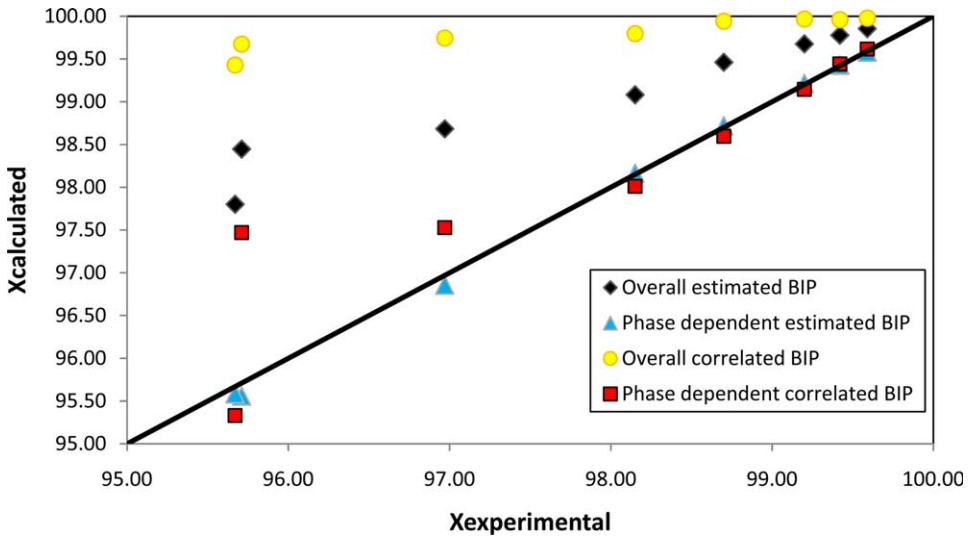

Figure 5. HPS overhead ethylene composition. Experimental and predicted data using overall and phase-dependent estimated and correlated BIP. [Color figure can be viewed in the online issue, which is available at wileyonlinelibrary.com.]

Table X. HPS Bottom Polymer and Ethylene Model C**omposition** Errors[a]

Resin	Overall estimated BIP (Table VI)		Phase-dependent estimated BIP (Table VII)		Overall correlated BIP [eq. (7)]		Phase-dependent correlated BIP [eq. (5) and (6)]	
	Polym[b]	Ethyl[c]	Polym[b]	Ethyl[c]	Polym[b]	Ethyl[c]	Polym[b]	Ethyl[c]
LDPE-1	0.36	1.36	−0.01	−0.03	−1.19	8.55	0.61	−2.01
LDPE-2	0.47	1.80	0.01	0.03	−0.60	7.78	0.69	−2.44
LDPE-3	1.09	3.54	0.02	0.07	1.88	5.26	1.09	−5.18
LDPE-4	0.65	2.38	0.02	0.08	−0.01	7.85	−0.73	2.18
LDPE-5	5.31	12.47	−0.31	−0.82	−2.03	48.50	−1.23	22.19
LDPE-6	1.31	4.86	0.04	0.14	−1.70	23.58	−0.66	1.05
LDPE-7	3.48	9.65	−0.16	−0.40	1.77	32.72	−0.34	−2.51
LDPE-8	2.69	8.58	−0.18	−0.54	−0.92	32.32	−0.06	6.08

[a] *error*[%] = 100 (*exp* − calc)/exp.

[b] Polymer.

[c] Ethylene.

be lower than the operational value, resulting in a lower production than the real one, since the HPS top stream is recirculated to the reactor (stream F4 in Figure 1). Another two points must be highlighted. First, a significant improvement is observed when using phase-dependent estimated BIP (Table VII). This excellent performance can be observed in bottom and overhead for all components. Second, even the predictive correlations expressed by eqs. (5) and (6) show a significant improvement over the use of the overall BIP approach. When we compare the predictive correlation results for both approaches the superiority of the phase-dependent BIP is even greater.

It should be also emphasized that although relatively few experimental data (5 points in each separator, summing 10 data points for fitting the correlation of each phase) have been used, the model had still shown significant predictive behavior. As can be seen in Table X, the overall correlated BIP show a greater relative error for both components when compared with the overall estimated BIP or with phase-dependent BIP (estimated or correlated). This is also true regarding their predictive capability, as can be seen from the relative errors for resins 3, 5, and 6, especially in the overhead compositions shown in Table XI.

CONCLUSIONS

In order to simulate the flash HPS (high pressure separator) and LPS (low pressure separator) in a industrial polyethylene process, experimental plant data of LDPE (low-density polyethylene) resins were used to test the PC-SAFT (perturbed-chain statistical associating fluid theory) EOS (equation of state) performance. To obtain quantitative results the most confident values of binary interaction parameters (BIP) should be determined from comprehensive experimental data of well-characterized polymer

Table XI. HPS Overhead Ethane and Ethylene Model C**omposition** Errors[a]

Resin	Overall estimated BIP (Table VI)		Phase-dependent estimated BIP (Table VII)		Overall correlated BIP [eq. (7)]		Phase-dependent correlated BIP [eqs. (5) and (6)]	
	Etha[a]	Ethyl[c]	Etha[b]	Ethyl[c]	Etha[b]	Ethyl[c]	Etha[b]	Ethyl[c]
LDPE-1	58.51	−0.26	−6.61	0.01	93.70	−0.39	−9.73	−0.03
LDPE-2	56.86	−0.36	−6.93	−0.01	93.74	−0.54	−11.75	−0.02
LDPE-3	57.62	−0.77	−0.37	−0.02	95.48	−1.26	−10.48	0.11
LDPE-4	57.30	−0.48	−1.39	−0.01	94.45	−0.77	−10.66	0.06
LDPE-5	33.51	−2.86	−9.23	0.16	85.96	−4.14	−9.46	−1.84
LDPE-6	50.03	−0.95	−0.41	−0.01	89.82	−1.68	−9.40	0.14
LDPE-7	39.56	−2.23	−7.57	0.09	88.31	−3.93	−9.46	0.35
LDPE-8	42.11	−1.77	−8.61	0.12	89.48	−2.86	−9.94	−0.57

[a] *error*[%] = 100 (*exp* − calc)/exp.

[b] Ethane.

[c] Ethylene.

samples. The results obtained in this article emphasize the importance of the phase-dependent BIP in developing the calculation procedure for an ethylene-polyethylene system at high and low pressure and show how it can be used. One advantage of the improved BIP is the fact that they correctly predict phase behavior for both small molecules and polyethylene at LPS and HPS. However, more importantly they allow for wide-plant simulation consistency when composition-dependent BIP are used in polymer systems, a fact which should not be overlooked in many situations. Furthermore, we can express more accurately what is happening at each phase in terms of intermolecular forces as the intensity and nature of these forces are quite different and complex as can be seen elsewhere.[33]

Phase equilibrium BIP obtained through the predictive correlations developed in this work may be used for practical industrial purposes, i.e., in the conditions prevailing during the separation of ethylene-polyethylene mixture. In order to achieve better BIP predictions, and thus a better adjustment between experimental and calculated data using this approach, more experimental data are required.

ACKNOWLEDGMENTS

The financial support of Conselho Nacional de Desenvolvimento Científico e Tecnológico (CNPq) and Coordenação de Aperfeiçoamento de Pessoal de Nível Superior (CAPES) are gratefully acknowledged.

LIST OF SYMBOLS

A	Helmholtz free energy per number of mole
F	Mass flow rate
HPS	High-Pressure Separator
k	Binary Interaction Parameter [BIP, Equation (3)]
LPS	Low-Pressure Separator
m	Segment number
M	Average molecular weight (number)
M	Average molecular weight (mass)
MWD	Molecular Weight Distribution
O	Objective function
P	Pressure
PDI	Polydispersity index
T	Temperature
w	Weight fraction

Greek Letters

α, β, γ, δ	Constants in eqs. (5)–(7)
ϵ	Dispersion energy parameter
η, w, θ	Constants in eqs. (5)–(7)
k	Boltzmann Constant
ρ	Solid polymer density
σ	Segment diameter

Superscripts

assoc	Associative
calc	Calculated
disp	Dispersive
exp	Experimental
hc	Hard-chain
res	Residual
‘	Mass composition in the heavy phase
“	Mass composition in the light phase

Subscripts

i	Component i
j	Component j

REFERENCES

1. Bogdanovic, V.; Tasic, A.; Djordjevic B. *Ind. Eng. Chem. Process Des. Dev.* **1985**, *24*, 576.
2. Orbey, H.; Bokis, C. P.; Chen, C.-C. *Ind. Eng. Chem. Res.* **1998**, *37*, 4481.
3. Jog, P. K.; Chapman, W. G.; Gupta, S. K.; Swindoll, R. D. *Ind. Eng. Chem. Res.* **2002**, *41*, 887.
4. Chapman, W. G.; Gubbins, K. E.; Jackson, G.; Radosz, M. *Ind. Eng. Chem. Res.* **1990**, *29*, 1709.
5. de Loos, T. W.; de Graaf, L. J.; de Swaan Arons, J. *Fluid Phase Equilib.* **1996**, *117*, 40.
6. Sanchez, I. C.; Lacombe, R. H. *Macromolecules* **1978**, *11*, 1145.
7. Gauter, K.; Heidemann, R. A. *Fluid Phase Equilib.* **2001**, 183–184, *87*.
8. Krenz, R.; Laursen, T., Heidemann, R. A. *Ind. Eng. Chem. Res.* **2009**, *48*, 10664.
9. Nagy, I.; de Loos, T. W.; Krenz, R. A.; Heidemann, R. A. *J. Supercritical Fluids* **2006**, *37*, 115.
10. Sako, T.; Wu, A. H.; Prausnitz, J. M. *J. Appl. Polym. Sci.* **1989**, *38*, 1839.
11. Tork, T.; Sadowski, G.; Arlt, W.; Haan, A.; Krooshof, G. *Fluid Phase Equilib.* **1999**, *163*, 79.
12. Kontogeorgis, G. M.; Harismiadis, V. I.; Fredenslund, A.; Tassios, D. P. *Fluid Phase Equilib.* **1994**, *96*, 65.
13. Orbey, N.; Sandler, S. I. *AIChE J.* **1994**, *40*, 1203.
14. Peng, D. Y.; Robinson, D. B. *Ind. Eng. Chem. Fundam.* **1976**, *15*, 59.
15. Wong, D. S. H.; Sandler, S. I. *AIChE J.* **1992**, *38*, 671.
16. Huron, M. J.; Vidal, J. *Fluid Phase Equilib.* **1979**, *3*, 255.
17. Orbey, H.; Bokis, C. P.; Chen, C.-C. *Ind. Eng. Chem. Res.* **1998**, *37*, 1567.
18. Paricaud, P.; Galindo, A.; Jackson, G. *Ind. Eng. Chem. Res.* **2004**, *43*, 6871.
19. Costa, G.; Dias, T. S.; Cardoso, M. M.; Pereira, Y.; Pessoa, F. L. P.; Vieira de Melo, S. A. B.; Embiruçu, M. *Fluid Phase Equilib.* **2008**, *267*, 140.
20. Gross, J.; Sadowski, G. *Ind. Eng. Chem. Res.* **2001**, *40*, 1244.
21. Gross, J.; Sadowski, G. *Ind. Eng. Chem. Res.* **2002**, *41*, 5510.
22. Guerrieri, Y. Modeling and Simulation of Phase Equilibria in Polyethylene Plants Using PC-SAFT Equation of State. Master Thesis (In Portuguese), FEQ-UNICAMP, **2007**.
23. Tumakaka, F.; Sadowski, G. *Fluid Phase Equilibria* **2004**, *217*, 233.
24. Tumakaka, F.; Gross, J.; Sadowski, G. *Fluid Phase Equilibria* **2005**, *228*, 89.

25. Spyriouni, T.; Economou, I. G. *Polymer* **2005**, *46*, 10772.
26. Cheluget, E. L.; Bokis, C. P.; Wardhaugh, L.; Chen, C.-C.; Fisher, J. *Ind. Eng. Chem. Res.* **2002**, *41*, 968.
27. von Solms, N.; Kouskoumvekaki, I. A.; Michelsen, M. L.; Kontogeorgis, G. M. *Fluid Phase Equilibria* **2006**, *241*, 344.
28. Kouskoumvekaki, I. A.; von Solms, N.; Michelsen, M. L.; Kontogeorgis, G. M. *Fluid Phase Equilibria* **2004**, *215*, 71.
29. von Solms, N.; Kouskoumvekaki, I. A.; Lindvig, T.; Michelsen, M. L.; Kontogeorgis, G. M. *Fluid Phase Equilibria* **2004**, *222*, 87.
30. Tihic, A.; Kontogeorgis, G. M.; von Solms, N.; Michelsen, M. L.; Constantinou, L. A. *Ind. Eng. Chem. Res.* **2008**, *47*, 5092.
31. Tihic, A.; von Solms, N.; Michelsen, M. L.; Kontogeorgis, G. M.; Constantinou, L. *Fluid Phase Equilib.* **2009**, *281*, 70.
32. Buchelli, A.; Call, M. L.; Brown, A. L.; Bokis, C. P.; Ramanathan, S.; Franjione, J. *Ind. Eng. Chem. Res.* **2004**, *43*, 1768.
33. Haslam, A. J.; Galindo, A.; Jackson, G. *Fluid Phase Equilib.* **2008**, *266*, 105.
34. Nelder, J. A.; Mead, R. *Comput. J.* **1964**, *7*, 308.
35. Costa, G. M. N.; Guerrieri, Y.; Kislansky, S.; Vieira de Melo, S. A. B.; Embiruçu, M.; Pessoa, F. L. P. *Comput.-Aided Chem. Eng.* **2009**, *27*, 405.
36. Embiruçu, M.; Prata, D. M.; Lima, E. L.; Pinto, J. C. *Macrom. Reac. Eng.* **2008**, *2*, 142.
37. Costa, G. M. N.; Guerrieri, Y.; Kislansky, S.; Pessoa, F. L. P.; Vieira de Melo, S. A. B.; Embiruçu, M. *Ind. Eng. Chem. Res.* **2009**, *48*, 8613.
38. Costa, G. M. N.; Kislansky, S.; Oliveira, L. C.; Pessoa, F. L. P.; Vieira de Melo, S. A. B.; Embiruçu, M. *J. Appl. Polym. Sci.* **2011**, *121*, 1832.
39. Costa, G. M. N.; Kislansky, S.; Guerrieri, Y.; Pessoa, F. L. P.; Vieira de Melo, S. A. B.; Embiruçu, M. *Ind. Eng. Chem. Res.* **2010**, *49*, 12242.
40. Wohlfarth, C.; Rätzsch, M. T. *Acta Polymerica* **1981**, *32*, 733.
41. Van Ness, H. C.; Abbott, M. M. Classical Thermodynamics of Nonelectrolyte Solutions with Application to Phase Equilibria; McGraw-Hill Book Company: New York, NY, **1982**.

APPENDIX A: The most general form of the Gibbs-Duhem equation applied to any molar property M in a homogeneous phase is given by:

$$\left(\frac{\partial M}{\partial T}\right)_{P,x}\cdot dT+\left(\frac{\partial M}{\partial P}\right)_{T,x}\cdot dP-\sum\nolimits_i \bar{x}_i\cdot d\bar{M}_i=0 \tag{A1}$$

We are using different binary interaction parameters for each phase in equilibrium, so the Gibbs-Duhem equation should not be used, but rather a relationship between the properties in equilibrium phases. This can be expressed as:

$$\hat{f}_i^{\,v}=\hat{f}_i^{\,l} \tag{A2}$$

It is unnecessary the study of the fugacity variation with regard to composition and temperature because there is agreement in the scientific community about this issue. Therefore, the unconventional variable used in this development of a BIP correlation is the pressure. An alternative to this assessment is the study of pressure variation in equilibrium relationship expressed by eq. (A3):[41]

$$\left(\frac{\partial \ln \hat{f}_i}{\partial P}\right)_{T,x}=\frac{\bar{v}_i}{R\cdot T} \tag{A3}$$

Taking into account eqs. (A2) and (A3) the following identity must be satisfied:

$$\bar{v}_i^{L}(P,T,\{x_i\})=\bar{v}_i^{V}(P,T,\{y_i\}) \tag{A4}$$

It is observed that this analysis was performed regardless of the equation of state used to describe the equilibrium.

Since eq. (A4) must be satisfied regardless of the equation of state used to describe the equilibrium, and due to the complexity of PC-SAFT equation to express the partial molar volume of component i in the mixture, it was chosen a simpler model [Peng-Robinson EOS, eq. (A5), with mixing rules given by eqs. (A6), (A7), and (A8)] to demonstrate the consistency of using pressure-dependent BIP.

$$P=\frac{R\cdot T}{v-b}-\frac{a}{v^2+2\cdot b\cdot v-b^2} \tag{A5}$$

$$a=\sum_i\sum_j x_i^{\,i}\cdot x_j\cdot a_{ij} \tag{A6}$$

$$a_{ij}=\sqrt{a_i\cdot a_j}\cdot\left(1-k_{ij}\right) \tag{A7}$$

$$b=\sum_i x_i\cdot b_i \tag{A8}$$

It can be shown that for this equation of state with these mixing rules the following expression can be obtained for the partial molar volume of component i:

$$\bar{v}_i=\left\{\frac{R\cdot T}{(v-b)}\cdot\left[1+\frac{b_i}{(v-b)}\right]-\frac{2\cdot\sum_k y_k\cdot\sqrt{a_i\cdot a_j}\cdot\left(1-K_{ij}\right)}{(v^2+2\cdot b\cdot v-b^2)}+\frac{a\cdot(v-b)\cdot 2\cdot b_i}{(v^2+2\cdot b\cdot v-b^2)^2}\right\}\cdot\cdot\left[\frac{R\cdot T}{(v-b)^2}-\frac{2\cdot a\cdot(v+b)}{(v^2+2\cdot b\cdot v-b^2)}\right]^{-1} \tag{A9}$$

As can be seen, by substituting eq. (A9) into eq. (A4), in order that this equation is satisfied, there is no numeric or conceptual obstacle that the interaction parameter is dependent on the pressure. It must also be noted that the compositions of the phases are different and therefore different functional relationships must be written for each phase at any time without infringing equality expressed by eq. (A4).